Dimensional Analysis and simplifications of a Mathematical Model describing High-Pressure Food Processes

Nadia Smith, Ángel Manuel Ramos

Departamento de Matemática Aplicada, Universidad Complutense de Madrid

nas.smith@mat.ucm.es, http://www.mat.ucm.es/~aramosol

Sarah Mitchell

Department of Mathematics & Statistics, University of Limerick

http://www.staff.ul.ie/mitchells/index.html

Abstract

Nowadays, consumers look for minimally processed, additive-free food products that maintain their organoleptic properties. This has promoted the development of new technologies for food processing. One emerging technology is high hydrostatic pressure, as it proves to be very effective in prolonging the shelf life of foods without losing its properties. Recent works have been done on the modelling and simulation of the effect of the combination of thermal and high pressure processes. These focus mainly on the inactivation that occurs during the process of certain enzymes and microorganisms that are harmful to food. Various mathematical models that study the behavior of these enzymes and microorganisms during and after the process have been proposed. Such models need as an input the temperature and pressure profiles of the whole process. In this work we present some of the existent two dimensional models to calculate the temperature profile for solid type foods and we propose a simplification to a one dimensional model.

The temperature profile of the one dimensional model is calculated both numerically and analytically, and these solutions are compared to the resulting temperature profile of the two dimensional model. This dimensional reduction is reasonable to do in some cases, which are specified in this work.

Sección en el CEDYA 2011: MAI

1 Introduction

There has been significant interest in the study of food engineering from the mid-twentieth century onwards (see, e.g., [21, 26]). Obviously, humans have been interested in food conservation since ancient times, using traditional techniques such as desiccation, conservation in oil, salting, smoking, cooling, etc. Due to the massive movement of populations to cities, a great supply of food in adequate conditions was necessary. Therefore, the food industry was developed in order to guarantee large-scale food techniques, to prolong its shelf life, and to make logistic aspects such as transport, distribution and storage, easier.

Classical industrial processes are based on thermal treatments. For example, pasteurization, sterilization and freezing. The disadvantage of classical freezing is non-homogeneous crystallization, which produces big crystals that may damage the food. For classical heat application processes, temperature is in a range of 60 to 120°C, and the processing time can vary from a few seconds to several minutes. The main aim of these processes is to inactivate microorganisms and enzymes that are harmful to food, in order to prolong its shelf life, to maintain or even to improve its natural qualities, and mainly to provide consumers with products in good condition. The problem of processing food via thermal treatments is that it may loose a significant part of its nutritional and organoleptic properties. At present, consumers look for minimally processed, additive-free food products that maintain such properties. Therefore the development of new technologies with lower processing temperatures has increased notoriously in the past years.

One of the new emerging technologies in this field is the combination of thermal treatments (at moderate temperatures) with high hydrostatic pressure, thereby reducing the problems described above. Many companies are using this technology and it is in increasing demand in countries such as Japan, USA and UK. Recent studies [4, 24] have proven that high pressure causes inactivation[1] of enzymes and microorganisms in food, while leaving small molecules (such as flavor and vitamins) intact, and therefore it does not modify significantly the organoleptic properties of the food. High pressure can also be used for freezing, resulting in uniform nucleation and crystallization. Our aim is to model mathematically these high pressure processes, in order to simulate and optimize them.

Two principles underlie the effect of high pressure. Firstly, the Le Chatelier Principle, according to which any phenomenon (phase transition, chemical reaction, chemical reactivity, change in molecular configuration) accompanied by a decrease in volume will be enhanced by pressure. Secondly, pressure is instantaneously and uniformly transmitted independently of the size and the geometry of the food (isostatic pressure).

Modelling and simulation of the effect of the combination of high pressure and thermal treatments on food processing has been carried out in [11], focusing on the temperature distribution and how to use this as an input for some models of inactivation of certain enzymes. In such work they consider both solid and liquid type foods. The complexity needed to solve the models (which include heat and mass transfer and non-constant thermophysical properties) can be very high. In this study, in which we focus only on solid type foods, we have performed dimensional analysis and seen that in some cases the models can be simplified (in dimension) and still work well. These models are very important in order to design suitable industrial equipments and optimize the processes.

In Section 2 the model to calculate the temperature distribution of a solid type food is presented. In Section 3 we simplify this model by performing

[1] **Inactivation** may be defined as the reduction of undesired biological activity, such as enzymatic catalysis and microbial contamination.

the dimensional analysis. In Section 4 we present some numerical results of the processes with the full model and compare them to those of the simplified model. In Section 5 we outline the final remarks.

Notation

C_p	Specific heat		*Greek symbols*
H	Domain height	β	Thermal expansion coeff.
h	Heat transfer coefficient	Γ	Whole domain bdry
k	Thermal conductivity	Γ_{r}	Known temperature bdry
L	Domain width	Γ_{up}	Heat transfer boundary
M	Mass	ρ	Density
$\mathbf{n}$	Outward normal unit vector	Ω	Domain of the device
P	Pressure		
r	Radial coordinate		*Indices*
t	Time	$*$	Rotated domain
t_{f}	Final time	$\hat{}$	Non dimensional variable
T	Temperature	0	Initial value
T_{env}	Environment Temperature	ref	Reference value
T_{r}	Refrigeration or heating temperature	C	Rubber cap
V	Volume	F	Food sample
z	Vertical coordinate	P	Pressurizing fluid
		S	Steel

2 Heat Transfer Modelling

When high pressure is applied in food technology, it is necessary to take into account the thermal effects that are produced by variations of temperature due to the compression/expansion that takes place in the food sample and the pressurizing medium. In practice, the pressure evolution, $P(t)$, is known as it is imposed by the user and the limits of the equipment. The temperature of the processed food may change with time and with space, therefore we need a heat transfer model capable of predicting the temperature for the processed food. Following [11], a heat transfer model taking into account only conduction effects is presented (for models also including convection effects see [11]). As the model is both time and spatially dependent, we also introduce a brief description of the domain describing the high pressure device considered in our simulations.

Usually HP experiments on food are carried out in a cylindrical pressure vessel (typically a hollow steel cylinder) that is filled with the food and the pressurizing fluid. We assume, due to the characteristics of this kind of processes, axial symmetry, which allows the use of cylindrical coordinates, and consider a two-dimensional domain with half a cross section (see Figure 1). The following four sub-domains are specified:

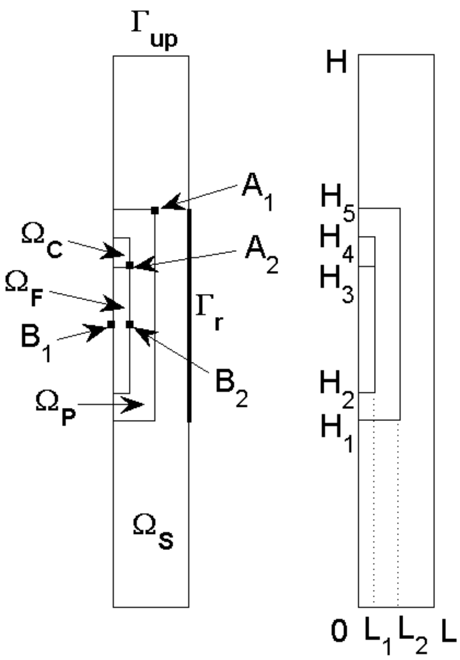

Figure 1: Computational domain

- $\Omega_{\rm F}$: domain that contains the food sample.
- $\Omega_{\rm C}$: cap of the sample holder (typically rubber).
- $\Omega_{\rm P}$: domain occupied by the pressurizing medium.
- $\Omega_{\rm S}$: domain of the steel that surrounds the rest of the domains.

The domain in the (r, z)-coordinates is the rectangle $\Omega = [0, L] \times [0, H]$ defined by $\overline{\Omega} = \overline{\Omega_{\rm F} \cup \Omega_{\rm C} \cup \Omega_{\rm P} \cup \Omega_{\rm S}}$. The boundary of Ω is denoted by Γ, where we can distinguish

- $\Gamma_{\rm r} \subset \{L\} \times [0, H]$, where the temperature is known.
- $\Gamma_{\rm up} = [0, L] \times \{H\}$, where heat transfer with the room in which equipment is located may take place.
- $\Gamma \setminus \{\Gamma_{\rm r} \cup \Gamma_{\rm up}\}$, that has zero heat flux, either by axial symmetry or by isolation of the equipment.

We use star notation ($[\ ]^*$) to denote the 3D domains generated by rotating all the domains explained above along the axis of symmetry ($\{0\} \times (0, H)$).

For the mathematical modelling two significantly different cases can be studied: solid and liquid type foods. In this paper, we only study solid type foods with a large filling ratio, and therefore a model that only takes into account conduction effects (and not convection effects) can give quite precise results (see [11, 23]).

2.1 Heat transfer by conduction

When solid type foods are considered, the starting point is the heat conduction equation for temperature T (K)

$$\rho C_p \frac{\partial T}{\partial t} - \nabla \cdot (k \nabla T) = \beta \, \frac{\mathrm{d}P}{\mathrm{d}t} \, T \ \text{ in } \Omega^* \times (0, t_\mathrm{f}), \tag{1}$$

where ρ is the density (kg m^{-3}), C_p the specific heat (J kg^{-1} K^{-1}), k the thermal conductivity (W m^{-1} K^{-1}) and t_f is the final time (s). The right hand side of equation (1) is the heat production due to the change of pressure $P = P(t)$ (Pa) applied by the equipment (chosen by the user within the machine limitations) and β is the thermal expansion coefficient, that is given by

$$\beta = \begin{cases} \beta_\mathrm{F} : \ \text{thermal expansion coefficient (K}^{-1}\text{) of the food in } \Omega^*_\mathrm{F}, \\ \beta_\mathrm{P} : \ \text{thermal expansion coefficient (K}^{-1}\text{) of the pressurizing fluid in } \Omega^*_\mathrm{P}, \\ 0, \ \text{elsewhere.} \end{cases}$$

This term results from the following law

$$\frac{\Delta T}{\Delta P} = \frac{\beta T V}{M C_p} = \frac{\beta T}{\rho C_p}, \tag{2}$$

where ΔT denotes the temperature change due to the pressure change ΔP, V is the volume and M the mass.

Equation (1) has to be completed with appropriate boundary and initial conditions depending on the HP machine and the problem we are wanting to solve. We use the same conditions as in Ref. [23] for a pilot unit (ACB GEC Alsthom, Nantes, France) located at the Instituto del Fro, CSIC, Spain

$$\begin{cases} k \dfrac{\partial T}{\partial \mathbf{n}} = 0 & \text{on} \quad \big(\Gamma^* \setminus (\Gamma^*_\mathrm{r} \cup \Gamma^*_\mathrm{up})\big) \times (0, t_\mathrm{f}), \\ k \dfrac{\partial T}{\partial z} = h(T_\mathrm{env} - T) & \text{on} \quad \Gamma^*_\mathrm{up} \times (0, t_\mathrm{f}), \\ T = T_\mathrm{r} & \text{on} \quad \Gamma^*_\mathrm{r} \times (0, t_\mathrm{f}), \\ T = T_0 & \text{in} \quad \Omega^* \times \{0\}, \end{cases} \tag{3}$$

where $\mathbf{n}$ is the outward unit normal vector on the boundary of the domain, T_0 is the initial temperature, T_r is the refrigeration or heating temperature that is constant on Γ^*_r (cooling or warming the food sample), T_env is the environment temperature (constant) and h (W m^{-2} K^{-1}) is the heat transfer coefficient.

By using cylindrical coordinates and taking into account axial symmetry, system (1), (3) may be rewritten as the following 2D problem

$$\begin{cases} \rho\, C_p\, \dfrac{\partial T}{\partial t} - \dfrac{1}{r}\dfrac{\partial}{\partial r}\left(rk\dfrac{\partial T}{\partial r}\right) - \dfrac{\partial}{\partial z}\left(k\dfrac{\partial T}{\partial z}\right) = \beta\, \dfrac{\mathrm{d}P}{\mathrm{d}t}\, T & \text{in} \quad \Omega \times (0, t_{\mathrm{f}}), \\ k\dfrac{\partial T}{\partial \mathbf{n}} = 0 & \text{on} \quad (\Gamma \setminus (\Gamma_{\mathrm{r}} \cup \Gamma_{\mathrm{up}})) \times (0, t_{\mathrm{f}}), \\ k\dfrac{\partial T}{\partial z} = h(T_{\mathrm{env}} - T) & \text{on} \quad \Gamma_{\mathrm{up}} \times (0, t_{\mathrm{f}}), \\ T = T_{\mathrm{r}} & \text{on} \quad \Gamma_{\mathrm{r}} \times (0, t_{\mathrm{f}}), \\ T = T_0 & \text{in} \quad \Omega \times \{0\}. \end{cases} \tag{4}$$

This model is suitable when the filling ratio of the food sample inside the vessel is much higher than that in the pressurizing medium, since convection effects due to the pressurizing fluid have been neglected. This has been confirmed to be true in [23], by validation with several comparisons between numerical and experimental results. They also show that when the filling ratio of the food inside the vessel is not much higher than in the pressurizing medium, the solution of this model differs a lot from the experimental results. Therefore they improve the model by including convection effects in the pressurizing medium. This case will not be studied in the present paper. In this paper, according to Figure 1 we assume $H_2 = H_1$ and L_1 to be very close to L_2.

In the following sections we study if it is possible to reduce the model for solid food with large filling ratio in two dimensions, to a simpler one-dimensional model. As explained above, to do so we perform dimensional analysis of system (4) and also compare the two dimensional models to the one dimensional ones, using numerical tests.

3 Dimensional analysis

We perform dimensional analysis to determine which terms may be neglected in the governing equation. We non-dimensionalise the equations of system (4) using the following scales (the symbol ˆ denotes non-dimensional variables):

$$\hat{r} = \frac{r}{R}, \qquad \hat{z} = \frac{z}{Z}, \qquad \hat{t} = \frac{t}{\tau}, \qquad \hat{T} = \frac{T - T_{\mathrm{r}}}{\Delta T},$$

where ΔT, R, Z and τ are the temperature, radius, height and time scales, resp., for significant temperatures variations within the food.

Given that in equation (4), the pressure function only appears in a derivative form, and that the pressure applied on these processes is a linear function in time (hence such derivative is usually piecewise constant) we do not non-dimensionalise the pressure variable (in order to simplify the analysis). Instead, we rewrite the pressure derivative $\frac{\mathrm{d}P}{\mathrm{d}t}(t)$ as

$$\frac{\mathrm{d}P}{\mathrm{d}t}(t) = \begin{cases} \dfrac{\gamma}{t_p}, & 0 < t \leq t_p, \\ 0, & t > t_p, \end{cases} \tag{5}$$

where, for the sake of simplicity, we suppose that $\frac{\mathrm{d}P}{\mathrm{d}t}(t) = \frac{\gamma}{t_p} > 0$ (P linear) for all $t \in [0, t_\mathrm{f}]$, and γ (Pa) is the maximum pressure reached. After time t_p the pressure is maintained constant at the maximum value, and therefore the derivative is zero (other cases can be also studied similarly).

Therefore, for $0 < t \leq t_p$ the first equation of (4) can be written as

$$\rho\, C_p\, \frac{\partial T}{\partial t} - \frac{1}{r}\frac{\partial}{\partial r}\left(rk\frac{\partial T}{\partial r}\right) - \frac{\partial}{\partial z}\left(k\frac{\partial T}{\partial z}\right) = \beta\, \frac{\gamma}{t_p}\, T \tag{6}$$

and for $t_p < t \leq t_\mathrm{f}$ the same equation holds, with the right-hand side equal to zero. We now write (6) in non-dimensional variables, that for $0 < \hat{t} \leq \frac{t_p}{\tau}$, becomes

$$\frac{\rho\, C_p\, \Delta T}{\tau}\frac{\partial \hat{T}}{\partial \hat{t}} - \frac{k\Delta T}{R^2 \hat{r}}\frac{\partial}{\partial \hat{r}}\left(\hat{r}\frac{\partial \hat{T}}{\partial \hat{r}}\right) - \frac{k\Delta T}{Z^2}\frac{\partial^2 \hat{T}}{\partial \hat{z}^2} = \frac{\beta\gamma\Delta T}{t_p}(\hat{T} + \frac{T_\mathrm{r}}{\Delta T}). \tag{7}$$

For ease of notation, from now on we drop the ˆ notation; therefore, in this section, T, z, r and t are now the non-dimensional variables.

All the coefficients in equation (7) have the same dimensions, that are (in dimensional units): mass $\cdot$length^{-1} $\cdot$time^{-3}. Therefore dividing the equation by any of these coefficients will make all the groups of parameters dimensionless. We divide equation (7) by $\rho C_p \Delta T/\tau$, resulting in

$$\frac{\partial T}{\partial t} - \frac{k\tau}{R^2\rho C_p}\frac{\partial}{\partial r}\left(r\frac{\partial T}{\partial r}\right) - \frac{k\tau}{Z^2\rho C_p}\frac{\partial^2 T}{\partial z^2} = \frac{\beta\gamma\tau}{\rho C_p t_p}T + \frac{\beta\gamma\tau}{\rho C_p t_p}\frac{T_\mathrm{r}}{\Delta T}. \tag{8}$$

The dimensionless groups of parameters in equation (8) are

$$a = \frac{k\tau}{R^2\rho C_p}, \qquad b = \frac{k\tau}{Z^2\rho C_p}, \qquad c = \frac{\beta\gamma\tau}{\rho C_p t_p}, \qquad d = \frac{\beta\gamma\tau}{\rho C_p t_p}\frac{T_\mathrm{r}}{\Delta T}. \tag{9}$$

We are mainly interested in the temperature inside the food, therefore we take the following scales:

- $R = L_1$: the radius of the food sample holder.
- $Z = H_3 - H_2$: the height of the food sample holder.
- $\Delta T = \max\,\{|T_0 - T_\mathrm{r}|, \frac{\beta\gamma T_0}{\rho C_p}\}$, where ρ and C_p are the density and specific heat of the food sample, respectively. We point out that $\frac{\beta\gamma T_0}{\rho C_p}$ is the maximum increase of temperature in the food sample due to the increase of pressure (according to (2)).

- The time scale, τ, is yet to be determined. We want to study what happens when the pressure is increased and therefore balance the largest one of the group of parameters on the right-hand side of equation (8) (where the pressure appears) with the left-hand side (i.e. the coefficient of the time derivative of temperature). This leads to:

$$\tau = \frac{\rho C_p t_p}{\beta\gamma} \min \left\{1, \frac{\Delta T}{T_\mathrm{r}}\right\}.$$

With all the previously chosen scales, we can now rewrite system (4) in a simplified non-dimensional form:

$$\begin{cases} \dfrac{\partial T}{\partial t} - a\dfrac{1}{r}\dfrac{\partial}{\partial r}\left(r\dfrac{\partial T}{\partial r}\right) - b\dfrac{\partial^2 T}{\partial z^2} = (cT+d)\chi_{(0,\frac{t_p}{\tau})}(t) & \text{in} \quad \hat{\Omega} \times (0, \frac{t_\mathrm{f}}{\tau}), \\ \dfrac{\partial T}{\partial \mathbf{n}} = 0 & \text{on} \quad \left(\hat{\Gamma} \setminus (\hat{\Gamma}_\mathrm{r} \cup \hat{\Gamma}_\mathrm{up})\right) \times (0, \frac{t_\mathrm{f}}{\tau}), \\ b\dfrac{\partial T}{\partial z} = \dfrac{hbZ}{k}(T^* - T) & \text{on} \quad \hat{\Gamma}_\mathrm{up} \times (0, \frac{t_\mathrm{f}}{\tau}), \\ T = 0 & \text{on} \quad \hat{\Gamma}_\mathrm{r} \times (0, \frac{t_\mathrm{f}}{\tau}), \\ T = \dfrac{T_0 - T_\mathrm{r}}{\Delta T} & \text{in} \quad \hat{\Omega} \times \{0\}, \end{cases} \tag{10}$$

where

$$\chi_{(0,\frac{t_p}{\tau})}(t) = \begin{cases} 1, & \text{if} \quad t \in (0, \frac{t_p}{\tau}), \\ 0, & \text{elsewhere.} \end{cases}$$

$\hat{\Omega} = (0, \frac{L}{R}) \times (0, \frac{H}{Z})$ is the non-dimensional form of the whole domain Ω. $\hat{\Gamma}$, $\hat{\Gamma}_\mathrm{r}$ and $\hat{\Gamma}_\mathrm{up} = (0, \frac{L}{R}) \times \{\frac{H}{Z}\}$ are the non-dimensional forms of the boundaries Γ, Γ_r and Γ_up, respectively. T^* is the result of non-dimensionalising T_env, i.e. $T^* = \frac{T_\mathrm{env} - T_\mathrm{r}}{\Delta T}$. The constants a, b, c and d, defined in (9), are different in the regions corresponding to the non-dimensional forms of Ω_F, Ω_C, Ω_P and Ω_S, that are, resp., $\hat{\Omega}_\mathrm{F} = (0, \frac{L_1}{R}) \times (\frac{H_2}{Z}, \frac{H_3}{Z})$, $\hat{\Omega}_\mathrm{C} = (0, \frac{L_1}{R}) \times (\frac{H_3}{Z}, \frac{H_4}{Z})$, $\hat{\Omega}_\mathrm{P} = \big((0, \frac{L_2}{R}) \times (\frac{H_1}{Z}, \frac{H_5}{Z})\big) \setminus (\hat{\Omega}_\mathrm{F} \cup \hat{\Omega}_\mathrm{C})$, and $\hat{\Omega}_\mathrm{S} = ((0, \frac{L}{R}) \times (0, \frac{H}{Z})) \setminus (\hat{\Omega}_\mathrm{F} \cup \hat{\Omega}_\mathrm{C} \cup \hat{\Omega}_\mathrm{P})$. $\mathbf{n}$ is the outward unit normal vector on the boundary of the non-dimensional domain, i.e.

$$\mathbf{n} \in \{(\pm 1, 0), (0, -1)\},$$

depending on which part of the domain we are on.

From the physics of the problem, the cooling/heating of the food sample comes either from the adiabatic heat produced by the increase of pressure (homogeneous in the whole food sample) or from the boundary condition. It therefore seems reasonable to assume that, if R is significantly smaller than Z, heat will flow in the radial direction rather than in the height direction. Thus, we are interested in studying if the heat transfer due to conduction is dominant in the radial direction over the height direction. We will do this using asymptotic expansion techniques.

Let $\varepsilon = \frac{R}{Z}$, then $b = \varepsilon^2 a$ and system (10) can be rewritten as

$$\begin{cases} \dfrac{\partial T}{\partial t} - a\dfrac{1}{r}\dfrac{\partial}{\partial r}\left(r\dfrac{\partial T}{\partial r}\right) - a\varepsilon^2\dfrac{\partial^2 T}{\partial z^2} = (cT+d)\chi_{(0,\frac{t_p}{\tau})}(t) & \text{in} \quad \hat{\Omega}\times(0,\frac{t_f}{\tau}), \\ \dfrac{\partial T}{\partial \mathbf{n}} = 0 & \text{on} \quad \left(\hat{\Gamma}\setminus(\hat{\Gamma}_{\mathrm{r}}\cup\hat{\Gamma}_{\mathrm{up}})\right)\times(0,\frac{t_f}{\tau}), \\ a\varepsilon\dfrac{\partial T}{\partial z} = \dfrac{haR}{k}(T^*-T) & \text{on} \quad \hat{\Gamma}_{\mathrm{up}}\times(0,\frac{t_f}{\tau}), \\ T = 0 & \text{on} \quad \hat{\Gamma}_{\mathrm{r}}\times(0,\frac{t_f}{\tau}), \\ T = \dfrac{T_0 - T_{\mathrm{r}}}{\Delta T} & \text{in} \quad \hat{\Omega}\times\{0\}, \end{cases} \tag{11}$$

We now suppose that the solution can be expanded in powers of ε. In other words,

$$T \sim T^{(0)} + \varepsilon T^{(1)} + \varepsilon^2 T^{(2)} + \cdots \tag{12}$$

and we assume that the expansions for the partial derivatives of T can be obtained by differentiating (12). Substituting (12) into (11), and equating coefficients of powers of ε at $O(1)$ (equivalent to putting $\varepsilon = 0$) we obtain

$$\begin{cases} \dfrac{\partial T^{(0)}}{\partial t} - a\dfrac{1}{r}\dfrac{\partial}{\partial r}\left(r\dfrac{\partial T^{(0)}}{\partial r}\right) = (c\,T^{(0)}+d)\chi_{(0,\frac{t_p}{\tau})}(t) & \text{in} \quad \hat{\Omega}, \\ \dfrac{\partial T^{(0)}}{\partial \mathbf{n}} = 0 & \text{on} \quad \left(\hat{\Gamma}\setminus(\hat{\Gamma}_{\mathrm{r}}\cup\hat{\Gamma}_{\mathrm{up}})\right), \\ T^{(0)} = T^* & \text{on} \quad \hat{\Gamma}_{\mathrm{up}}, \\ T^{(0)} = 0 & \text{on} \quad \hat{\Gamma}_{\mathrm{r}}, \\ T^{(0)} = \dfrac{T_0 - T_{\mathrm{r}}}{\Delta T} & \text{at} \quad t = 0. \end{cases} \tag{13}$$

System (13) must be solved in the three regions to determine the temperature in the food, T_{F}, temperature in the pressurizing fluid, T_{P}, and temperature in the steel, T_{S}. Thus, the system is described as follows (from now on we drop the $^{(0)}$ for ease of notation):

$$
\begin{cases}
\dfrac{\partial T_{\mathrm{F}}}{\partial t} - a_{\mathrm{F}}\dfrac{1}{r}\dfrac{\partial}{\partial r}\left(r\dfrac{\partial T_{\mathrm{F}}}{\partial r}\right) = (c_{\mathrm{F}}\ T_{\mathrm{F}} + d_{\mathrm{F}})\chi_{(0,\frac{t_p}{\tau})}(t) & \text{in} \quad (0, \frac{L_1}{R}) \times (0, \frac{t_{\mathrm{f}}}{\tau}), \\
\dfrac{\partial T_{\mathrm{P}}}{\partial t} - a_{\mathrm{P}}\dfrac{1}{r}\dfrac{\partial}{\partial r}\left(r\dfrac{\partial T_{\mathrm{P}}}{\partial r}\right) = (c_{\mathrm{P}}\ T_{\mathrm{P}} + d_{\mathrm{P}})\chi_{(0,\frac{t_p}{\tau})}(t) & \text{in} \quad (\frac{L_1}{R}, \frac{L_2}{R}) \times (0, \frac{t_{\mathrm{f}}}{\tau}), \\
\dfrac{\partial T_{\mathrm{S}}}{\partial t} - a_{\mathrm{S}}\dfrac{1}{r}\dfrac{\partial}{\partial r}\left(r\dfrac{\partial T_{\mathrm{S}}}{\partial r}\right) = 0 & \text{in} \quad (\frac{L_2}{R}, \frac{L}{R}) \times (0, \frac{t_{\mathrm{f}}}{\tau}), \\
\dfrac{\partial T_{\mathrm{F}}}{\partial r} = 0 & \text{on} \quad \{0\} \times (0, \frac{t_{\mathrm{f}}}{\tau}), \\
k_{\mathrm{F}}\dfrac{\partial T_{\mathrm{F}}}{\partial r} = k_{\mathrm{P}}\dfrac{\partial T_{\mathrm{P}}}{\partial r}, \quad T_{\mathrm{F}} = T_{\mathrm{P}}, & \text{on} \quad \{\frac{L_1}{R}\} \times (0, \frac{t_{\mathrm{f}}}{\tau}), \\
k_{\mathrm{P}}\dfrac{\partial T_{\mathrm{P}}}{\partial r} = k_{\mathrm{S}}\dfrac{\partial T_{\mathrm{S}}}{\partial r}, \quad T_{\mathrm{P}} = T_{\mathrm{S}}, & \text{on} \quad \{\frac{L_2}{R}\} \times (0, \frac{t_{\mathrm{f}}}{\tau}), \\
T_{\mathrm{S}} = 0 & \text{on} \quad \{\frac{L}{R}\} \times (0, \frac{t_{\mathrm{f}}}{\tau}), \\
T_{\mathrm{F}} = T_{\mathrm{F}_0},\ T_{\mathrm{P}} = T_{\mathrm{P}_0},\ T_{\mathrm{S}} = T_{\mathrm{S}_0} & \text{in} \quad (0, \frac{L}{R}), \times\{0\}.
\end{cases} \tag{14}
$$

where T_{F_0}, T_{P_0} and T_{S_0} are the non dimensional initial temperatures in the food, pressurizing fluid and steel, respectively.

We are interested in finding the temperature profile inside the food sample, T_{F}. However, since the boundary condition at $r = \frac{L_1}{R}$ depends on T_{P}, we have to solve the coupled system for T_{F}, T_{P} and T_{S}.

Assuming certain conditions on the coefficients of the system (in Section 4 we give a example where such conditions hold) we can find a one dimensional analytic approximation to the solution of problem (14). The conditions are the following:

$$
\begin{cases}
a_{\mathrm{S}} \approx 100 a_{\mathrm{F}} \\
k_{\mathrm{S}} \approx 100 k_{\mathrm{F}} \\
a_{\mathrm{F}} \approx a_{\mathrm{P}}, c_{\mathrm{F}} \approx c_{\mathrm{P}} \text{ and } d_{\mathrm{F}} \approx d_{\mathrm{P}} \\
d_{\mathrm{F}} \approx 100 c_{\mathrm{F}} \approx 100 a_{\mathrm{F}} \\
L_2 - L_1 << L T_{\mathrm{env}} = T_{\mathrm{r}}
\end{cases} \tag{15}
$$

Assuming that the food and pressurizing fluid have almost identical properties, and also that the domain occupied by the fluid is small compared to the whole domain, the first simplification is to join the food and pressurizing fluid into one combined region, using the parameters for the food. Therefore the problem reduces to

$$\begin{cases} \dfrac{\partial T_{\mathrm{F}}}{\partial t} - a_{\mathrm{F}} \dfrac{1}{r}\dfrac{\partial}{\partial r}\left(r\dfrac{\partial T_{\mathrm{F}}}{\partial r}\right) = (c_{\mathrm{F}}\ T_{\mathrm{F}} + d_{\mathrm{F}})\chi_{(0,\frac{t_p}{\tau})}(t) & \text{in} \quad (0, \frac{L_2}{R}) \times (0, \frac{t_{\mathrm{f}}}{\tau}), \\ \dfrac{\partial T_{\mathrm{S}}}{\partial t} - a_{\mathrm{S}} \dfrac{1}{r}\dfrac{\partial}{\partial r}\left(r\dfrac{\partial T_{\mathrm{S}}}{\partial r}\right) = 0 & \text{in} \quad (\frac{L_2}{R}, \frac{L}{R}) \times (0, \frac{t_{\mathrm{f}}}{\tau}), \\ \dfrac{\partial T_{\mathrm{F}}}{\partial r} = 0 & \text{on} \quad \{0\} \times (0, \frac{t_{\mathrm{f}}}{\tau}), \\ k_{\mathrm{F}}\dfrac{\partial T_{\mathrm{F}}}{\partial r} = k_{\mathrm{S}}\dfrac{\partial T_{\mathrm{S}}}{\partial r}, \quad T_{\mathrm{F}} = T_{\mathrm{S}}, & \text{on} \quad \{\frac{L_2}{R}\} \times (0, \frac{t_{\mathrm{f}}}{\tau}), \\ T_{\mathrm{S}} = 0 & \text{on} \quad \{\frac{L}{R}\} \times (0, \frac{t_{\mathrm{f}}}{\tau}), \\ T_{\mathrm{F}} = T_{\mathrm{F}_0},\ T_{\mathrm{S}} = T_{\mathrm{S}_0} & \text{in} \quad (0, \frac{L}{R}) \times \{0\}. \end{cases} \tag{16}$$

We first solve the problem in the steel region. Given that $k_{\mathrm{S}} \approx 100 k_{\mathrm{F}}$, we make the following simplification of the boundary condition on $r = \frac{L_2}{R}$:

$$\left(\frac{\partial T_{\mathrm{S}}}{\partial r}\right) = \frac{k_{\mathrm{F}}}{k_{\mathrm{S}}}\frac{\partial T_{\mathrm{F}}}{\partial r} \approx 0, \text{ on } r = \frac{L_2}{R}$$

and this implies that $T_{\mathrm{S}} \approx 0$ in the steel. We would like to remark that whilst doing this approximation we are also taking into account the fact that the steel has such a high thermal diffusivity, a_{S}. Therefore it goes to steady state very rapidly almost everywhere, and the solution to the steady state problem is zero. Then the boundary condition for T_{F} at $r = \frac{L_2}{R}$ (from now on we will call $\frac{L_2}{R} = L^*$, for ease of notation) is simply

$$T_{\mathrm{F}} = 0, \text{ on } r = L^*.$$

Thus we now only have the temperature in the food problem to solve, which reduces to

$$\begin{cases} \dfrac{\partial T_{\mathrm{F}}}{\partial t} - a_{\mathrm{F}} \dfrac{1}{r}\dfrac{\partial}{\partial r}\left(r\dfrac{\partial T_{\mathrm{F}}}{\partial r}\right) = (c_{\mathrm{F}}\ T_{\mathrm{F}} + d_{\mathrm{F}})\chi_{(0,\frac{t_p}{\tau})}(t) & \text{in} \quad (0, L^*) \times (0, \frac{t_{\mathrm{f}}}{\tau}), \\ \dfrac{\partial T_{\mathrm{F}}}{\partial r} = 0 & \text{on} \quad \{0\} \times (0, \frac{t_{\mathrm{f}}}{\tau}), \\ T_{\mathrm{F}} = 0 & \text{on} \quad \{L^*\} \times (0, \frac{t_{\mathrm{f}}}{\tau}), \\ T_{\mathrm{F}} = T_{\mathrm{F}_0} & \text{in} \quad (0, \frac{L}{R}) \times \{0\}. \end{cases} \tag{17}$$

We need to solve two different problems for the different time periods, i.e. $t \in (0, \frac{t_{\mathrm{p}}}{\tau})$ and $t \geq \frac{t_{\mathrm{p}}}{\tau}$. For time $t \in (0, \frac{t_{\mathrm{p}}}{\tau})$, heating occurs due to the increase of pressure. As $d_{\mathrm{F}} \approx 100 c_{\mathrm{F}} \approx 100 a_{\mathrm{F}}$, at leading order the equation reduces to

$$\frac{\partial T_{\mathrm{F}}}{\partial t} = d_{\mathrm{F}},\ t \in (0, \frac{t_{\mathrm{p}}}{\tau}),$$

which has the analytical solution

$$T_{\mathrm{F}}(t, r) = d_{\mathrm{F}} t + T_{\mathrm{F}_0}, \text{ for } t \in (0, \frac{t_{\mathrm{p}}}{\tau}). \tag{18}$$

However, solution (18) does not satisfy the boundary condition at $r = L^*$, and so we need a boundary layer of thickness δ, that is still to be determined. Setting

$$r = L^* - \delta \bar{r},$$

the first equation of (17) becomes

$$\frac{\partial T_{\mathrm{F}}}{\partial t} - \frac{a_{\mathrm{F}}}{\delta^2} \frac{1}{L^* - \delta \bar{r}} \frac{\partial}{\partial \bar{r}} \left((L^* - \delta \bar{r}) \frac{\partial T_{\mathrm{F}}}{\partial \bar{r}} \right) = (c_{\mathrm{F}}\ T_{\mathrm{F}} + d_{\mathrm{F}}) \chi_{(0, \frac{t_p}{\tau})}(t), \quad 0 < \bar{r} < \infty. \tag{19}$$

Taking $\delta = \sqrt{a_{\mathrm{F}}}$, (19) becomes, at leading order

$$\frac{\partial T_{\mathrm{F}}}{\partial t} - \frac{\partial^2 T_{\mathrm{F}}}{\partial \bar{r}^2} = d_{\mathrm{F}}, \quad 0 < \bar{r} < \infty, \tag{20}$$

and combined with the boundary condition leads to the following system:

$$\begin{cases} \dfrac{\partial T_{\mathrm{F}}}{\partial t} - \dfrac{\partial^2 T_{\mathrm{F}}}{\partial \bar{r}^2} = d_{\mathrm{F}} & \text{in} \quad 0 < \bar{r} < \infty, \times (0, \frac{t_{\mathrm{f}}}{\tau}), \\ T_{\mathrm{F}} = 0 & \text{on} \quad \bar{r} = 0, \\ T_{\mathrm{F}} \to T^{(\mathrm{out})} & \text{as} \quad \bar{r} \to \infty, \\ T_{\mathrm{F}} = T_{\mathrm{F}_0} & \text{at} \quad t = 0, \end{cases} \tag{21}$$

where $T^{(\mathrm{out})}$ is the outer solution given in (18). It is important to notice that $T^{(\mathrm{out})} = d_{\mathrm{F}} t + T_{\mathrm{F}_0}$ is a function that only depends on time. Equation (21) can be solved by taking Laplace transforms in t, and the solution is given by

$$G(\bar{r}, t) = t + T_{\mathrm{F}_0} - \left(T_{\mathrm{F}_0} + t + \frac{\bar{r}^2}{2} \right) \operatorname{erfc} \left(\frac{\bar{r}}{2\sqrt{t}} \right) + \sqrt{\frac{t}{\pi}} \bar{r} e^{-\frac{\bar{r}^2}{4t}}, \tag{22}$$

where $\operatorname{erfc}(\cdot)$ is the complementary error function.

Finally, we can write the boundary layer solution (21) as

$$T_{\mathrm{F}}^{(\mathrm{inn})}(\bar{r}, t) = G(\bar{r}, t) + t + T_{\mathrm{F}_0}. \tag{23}$$

The solution to the original problem (17) is the composite expansion which is determined by adding the inner and outer solutions and subtracting the common part. Thus,

$$T_{\mathrm{F}}(r, t) = t + T_{\mathrm{F}_0} - \left(T_{\mathrm{F}_0} + t + \left(\frac{L^* - r}{\sqrt{2 a_{\mathrm{F}}}} \right)^2 \right) \operatorname{erfc} \left(\frac{L^* - r}{2\sqrt{t a_{\mathrm{F}}}} \right) + \sqrt{\frac{t}{\pi}} \left(\frac{L^* - r}{\sqrt{a_{\mathrm{F}}}} \right) e^{-\left(\frac{L^* - r}{2\sqrt{t a_{\mathrm{F}}}} \right)^2}. \tag{24}$$

For $t \geq \frac{t_{\rm p}}{\tau}$, heating no longer occurs due to the increase of pressure, and hence the right-hand side of the first equation in (17) is zero. Rescaling time as $\psi = t - \frac{t_{\rm p}}{\tau}$, we have

$$\begin{cases} \dfrac{\partial T_{\rm F}}{\partial \psi} - a_{\rm F}\dfrac{1}{r}\dfrac{\partial}{\partial r}\left(r\dfrac{\partial T_{\rm F}}{\partial r}\right) = 0 & \text{in} \quad (0, L^*) \times (0, \frac{t_{\rm f}}{\tau} - \frac{t_{\rm p}}{\tau}), \\ \dfrac{\partial T_{\rm F}}{\partial r} = 0 & \text{on} \quad \{0\} \times (0, \frac{t_{\rm f}}{\tau}), \\ T_{\rm F} = 0 & \text{on} \quad \{L^*\} \times (0, \frac{t_{\rm f}}{\tau}), \\ T_{\rm F} = h(r) & \text{in} \quad (0, \frac{L}{R}) \times \{0\}, \end{cases} \tag{25}$$

where $h(r)$ is the initial condition given by the solution (24) at time $t = \frac{t_{\rm p}}{\tau}$.

Since $a_{\rm F} << 1$, at leading order, (25) reduces to

$$\frac{\partial T_{\rm F}}{\partial \psi} = 0, \ \ \psi \in \left(0, \frac{t_{\rm f}}{\tau} - \frac{t_{\rm p}}{\tau}\right), \tag{26}$$

which has the analytical solution

$$T_{\rm F}(r, \psi) = h(r), \ \text{ for } \psi \in \left(0, \frac{t_{\rm f}}{\tau} - \frac{t_{\rm p}}{\tau}\right). \tag{27}$$

Solution (27) does satisfy the boundary conditions, but it is constant in time which does not agree with experimental data (see [11]). To include time dependence we perform an asymptotic expansion in terms of the small parameter $a_{\rm F}$. Hence we seek a solution of the form

$$T_{\rm F}(r, \psi) = T_{\rm F}^{[0]} + a_{\rm F} T_{\rm F}^{[1]} + a_{\rm F}^2 T_{\rm F}^{[2]} + \cdots \tag{28}$$

and we assume that the expansions for the partial derivatives of $T_{\rm F}$ can be obtained by differentiating (28). Substituting (28) into (25), we obtain a system in which the temperature is expanded in powers of $a_{\rm F}$. The $O(1)$ problem is simply (26), and so the solution is given by (27), i.e.,

$$T_{\rm F}^{[0]}(r, \psi) = h(r). \tag{29}$$

Equating coefficients of powers of $a_{\rm F}$ at $O(a_{\rm F})$ we have

$$\begin{cases} \dfrac{\partial T_{\rm F}^{[1]}}{\partial \psi} - \dfrac{1}{r}\dfrac{\partial}{\partial r}\left(r\dfrac{\partial T_{\rm F}^{[0]}}{\partial r}\right) = 0 & \text{in} \quad (0, L^*) \times (0, \frac{t_{\rm f}}{\tau} - \frac{t_{\rm p}}{\tau}), \\ \dfrac{\partial T_{\rm F}^{[1]}}{\partial r} = 0 & \text{on} \quad \{0\} \times (0, \frac{t_{\rm f}}{\tau}), \\ T_{\rm F}^{[1]} = 0 & \text{on} \quad \{L^*\} \times (0, \frac{t_{\rm f}}{\tau}), \\ T_{\rm F}^{[1]} = 0 & \text{in} \quad (0, \frac{L}{R}) \times \{0\}. \end{cases} \tag{30}$$

As $T_{\mathrm{F}}^{[0]} = h(r)$, the first equation in (30) can be written as

$$\frac{\partial T_{\mathrm{F}}^{[1]}}{\partial \psi} = \frac{1}{r}(h'(r) + rh''(r)),$$

with solution

$$T_{\mathrm{F}}^{[1]}(r, \psi) = \frac{1}{r}(h'(r) + rh''(r))\psi.$$

Equating coefficients of powers of a_{F} at $O(a_{\mathrm{F}}^2)$, and repeating the same procedure, leads to

$$T_{\mathrm{F}}^{[2]}(r, \psi) = \left(\frac{h'(r)}{r^3} - \frac{h''(r)}{r^2} + 2\frac{h'''(r)}{r} + h^{IV}(r)\right)\frac{\psi^2}{2}.$$

Therefore, the solution for T_{F}, up to $O(a_{\mathrm{F}}^2)$, for $t \geq \frac{t_{\mathrm{f}}}{\tau}$, is given by

$$T_{\mathrm{F}}(r, t) = h(r) + a_{\mathrm{F}}\frac{1}{r}(h'(r) + rh''(r))\left(t - \frac{t_{\mathrm{f}}}{\tau}\right) + a_{\mathrm{F}}^2\left(\frac{h'(r)}{r^3} - \frac{h''(r)}{r^2} + 2\frac{h'''(r)}{r} + h^{IV}(r)\right)\frac{(t - \frac{t_{\mathrm{f}}}{\tau})^2}{2} \tag{31}$$

Combining (24) and (31) together, gives the solution to (17) for all times and together with $T_{\mathrm{S}} \approx 0$ we have the solution of system (16).

Recall that this is the first term, $T^{(0)}$, of the asymptotic expansion (12). Now we have to see if the boundary condition $T^{(0)} = T^*$ on $\hat{\Gamma}_{\mathrm{up}}$ in (13) holds for our solution $T^{(0)}$. Given that $T^* = \frac{T_{\mathrm{env}} - T_{\mathrm{r}}}{\Delta T}$ and one of our assumptions is that $T_{\mathrm{env}} = T_{\mathrm{r}}$, it follows that $T^* = 0$ and hence the solution $T_{\mathrm{S}} \approx 0$ does satisfy the boundary condition on $\hat{\Gamma}_{\mathrm{up}}$. If this were not the case we would have to look for boundary layers in the vertical direction, to ensure that the solution satisfies all the boundary conditions.

4 Numerical tests

For the numerical tests we have considered the size of the pilot unit (ACB GEC Alsthom, Nantes, France) that was used in [23]. The dimensions of the machine are given in Table 1. The numerical tests we present are computed in cylindrical coordinates (for the 2D model) and radial coordinates (for the 1D-model), in both cases assuming axial symmetry. We use the Finite Element Method (FEM) solver COMSOL Multiphysics 3.5a to compute the solutions.

In this section we compare the non dimensional equations presented in the previous section with the numerical solutions. For simplicity, we will assume that the thermophysical properties of the food, the pressurizing media, the steel and the rubber cap of the sample holder (i.e. in Ω_{F}, Ω_{P}, Ω_{S} and Ω_{C}, resp.) are constant (values are given in Table 1). We have chosen tylose as an example of solid type food and water as the pressurizing medium. We consider the following high pressure processes with different initial temperature and pressure curve (see [11]):

- Process P2: The initial temperature is $T_0 = 313$ K $= 39.85°$C in the whole domain Ω and the pressure is linearly increased (with the same slope as before) during the first 183 seconds until it reaches 360 MPa. Thus, the pressure generated by the equipment satisfies $P_2(0) = 0$ and

$$\frac{\mathrm{d}P_2}{\mathrm{d}t}(t) = \begin{cases} \dfrac{360}{183} \cdot 10^6 \text{ Pa s}^{-1}, & 0 < t \leq 183, \\ 0 \text{ Pa s}^{-1}, & t > 183. \end{cases} \tag{32}$$

$\rho_{\rm F}$	1006	$\rho_{\rm P}$	997	$\rho_{\rm S}$	7833	$\rho_{\rm C}$	1110	kg m^{-3}
$C_{p{\rm F}}$	3780	$C_{p{\rm P}}$	4179	$C_{p{\rm S}}$	465	$C_{p{\rm C}}$	1884	J kg^{-1} K^{-1}
$k_{\rm F}$	0.49	$k_{\rm P}$	0.613	$k_{\rm S}$	55	$k_{\rm C}$	0.173	W m^{-1} K^{-1}
$\beta_{\rm F}$	$4.217 \cdot 10^{-4}$	$\beta_{\rm P}$	$3.351 \cdot 10^{-4}$	K^{-1}		h	28	W m^{-2} K^{-1}
L_1	0.045	L_2	0.05	L	0.09	$H_1 = H_2$	0.222	m
H_3	0.404	H_4	0.439	H_5	0.472	H	0.654	m
$T_{0,2}$	295	t_{p_2}	183	$T_{\rm r}$	292.3	$T_{\rm env}$	292.3	K
$t_{\rm f}$	900	s	γ_2	$360 \cdot 10^6$	Pa			

Table 1: Typical parameter values for process with large filling ratio. The food properties are those of tylose and the pressurizing fluid those of water. Data obtained from [5, 11, 17].

Following the procedure described in Sec. 3 and considering the values given in Table 1, for process P_2, the values of the scales used to non-dimensionalise the variables are: $R = 0.045$ m, $Z = 0.182$ m, $\Delta T = 20.7$ K and $\tau = 325$ s. With these values, system (10) results in

$$\begin{cases} \dfrac{\partial T}{\partial t} - a\dfrac{1}{r}\dfrac{\partial}{\partial r}\left(r\dfrac{\partial T}{\partial r}\right) - b\dfrac{\partial^2 T}{\partial z^2} = (cT + d)\chi_{(0,0.56)}(t) & \text{in} \quad (0,2) \times (0,3.59) \times (0,2.76), \\ \dfrac{\partial T}{\partial \mathbf{n}} = 0 & \text{on} \quad \left(\hat{\Gamma} \setminus (\hat{\Gamma}_{\rm r} \cup \hat{\Gamma}_{\rm up})\right) \times (0,2.76), \\ \dfrac{\partial T}{\partial z} = -0.09T & \text{on} \quad \hat{\Gamma}_{\rm up} \times (0,2.76), \\ T = 0 & \text{on} \quad \hat{\Gamma}_{\rm r} \times (0,2.76), \\ T = 1 & \text{in} \quad (0,2) \times (0,3.59) \times \{0\}, \end{cases} \tag{33}$$

The values of a, b, c and d are shown in Table 2.

Figure 2 shows the temperature distribution of the solution of system (33) (converted back into dimensional units) inside the food sample. We can see that the differences in height are very small, but the differences in the radial coordinate are important.

In this case, in the food region, the non-dimensional coefficient of heat conduction along the height direction, i.e. b, has order $O(10^{-3})$ (see Table 2).

	a	b	c	d
$\hat{\Omega}_{\mathrm{F}}$	0.02	0.00126	0.07	1
$\hat{\Omega}_{\mathrm{P}}$	0.023	0.0014	0.05	0.7
$\hat{\Omega}_{\mathrm{C}}$	0.013	0.00081	0	0
$\hat{\Omega}_{\mathrm{S}}$	2.423	0.148	0	0

Table 2: Non-dimensional parameter values for system (33) for process P_2.

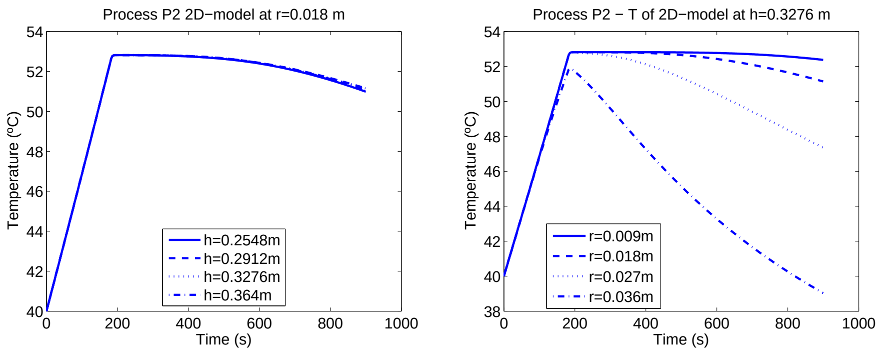

Figure 2: Process P_2. Temperature evolution (solution of 2D-model (33) in dimensional units) inside the food during a HP process at different heights and different radius.

Since the rest of the coefficients are of larger order, it suggests that the effects of the heat conduction along the height direction may be neglected inside the food sample. The numerical results agree with this conclusion (as shown in Figure 2), since the solution does not depend on the z-component. The left-hand side of Figure 2 shows the temperature inside the food at $r = 0.018$ m for different heights of the holder, and no significant differences are observed. The right-hand side of Figure 2 shows the temperature at $h = 0.3276$ m for different radial points, and important differences can be observed.

The non-dimensional and simplified 1D system of equations for the problem is therefore

$$\begin{cases} \dfrac{\partial T}{\partial t} - a\dfrac{1}{r}\dfrac{\partial}{\partial r}\left(r\dfrac{\partial T}{\partial r}\right) = (c\,T + d)\chi_{(0,0.56)}(t) & \text{in} \quad (0,2)\times(0,2.76), \\ \dfrac{\partial T}{\partial r} = 0 & \text{on} \quad \{0\}\times(0,2.76), \\ T = 0 & \text{on} \quad \{2\}\times(0,2.76), \\ T = 1 & \text{in} \quad (0,2)\times\{0\}, \end{cases} \tag{34}$$

where a, c and d are given in Table 2.

The left-hand side of Figure 3 is the result of solving the 1D-model (34)

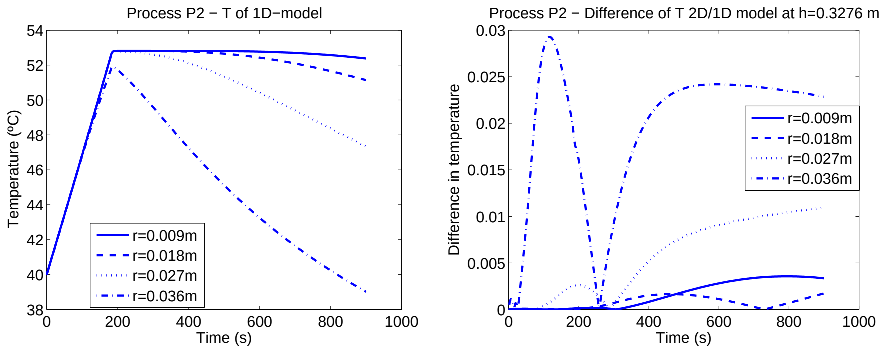

Figure 3: Process P_2. Left: Temperature evolution (solution of 1D-model (34) in dimensional units) inside food during a HP process at different radius. Right: Temperature differences between the 2D-model (33) at middle height and the 1D-model (34).

(converted back into dimensional units), and it is nearly identical to its respective two dimensional solution, i.e. the right-hand side of Figure 2, which plots the solution of the 2D-model (33). This shows again that the height dependence is negligible in nearly all the food domain. The right-hand side of Figure 3 shows the difference (very small) in temperatures between the 2D-model and the 1D-model at different radius and at mid height. However, when calculating such differences at a height near the top of the food sample (at $h = 0.396$ m) or at the bottom (at $h = 0.23$ m), they are not negligible. In Figure 4 we show the temperature differences of comparing the 2D-model to the 1D-model near the top and bottom of the food sample. These large differences have made us

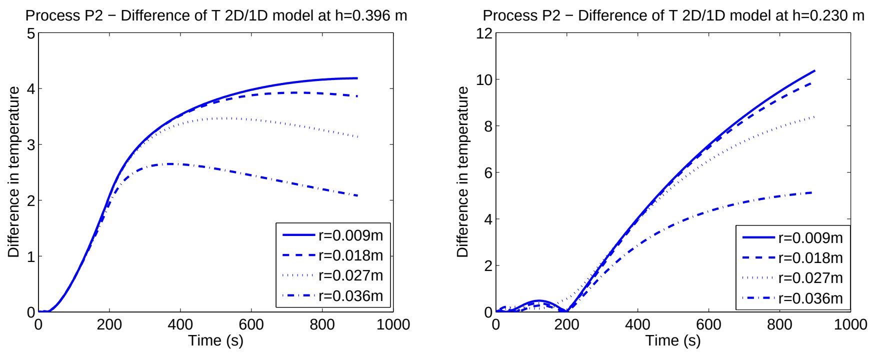

Figure 4: Process P_2. Temperature differences between the 2D-model (33) at nearly the top height (left), nearly the bottom height (right), and the 1D-model (34).

thought of the possibility of adding boundary layers near the top and bottom of the food sample to improve the 1D model, which will be done in future work.

Finally, we calculate the analytic solution of (34) as described in Section 3. The left-hand side of Figure 5 is the result of solving the 1D-model (34) (converted back into dimensional units) analytically. The right-hand side of Figure 5 shows the difference in temperatures between the numerical and analytical solution of the 1D-model (34). As can be seen the results are quite similar, which means that the analytical solution obtained from the asymptotic expansion is a good way of describing the solution.

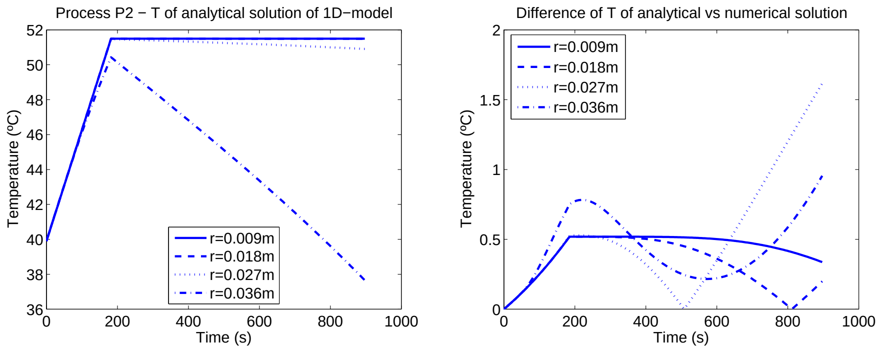

Figure 5: Process P_2. Temperature inside the food given by analytical solution (left) and temperature differences between the numerical and analytic solution of (34) (right).

5 Remarks

The mathematical models described in this paper provide a useful tool to design and optimize combined high pressure and thermal processes in Food Engineering when the processed food is a solid type food (for liquid type foods other models have to be considered, see e.g. [11]). They take into account the heat transfer and enzymatic or microbial inactivation occurring during the process.

Several simplified versions of the models have been proposed, namely, simplification of two dimensional heat transfer models to one dimensional ones, being motivated by the dimensional analysis also performed in this paper. When comparing such models, the results of the temperature evolution inside the food at nearly every point are quite similar. However, there are bigger differences if a point at the top or bottom of the food sample is considered. This is due to the fact that at a point near the top, the rubber cap of the food sample is very close, and the thermophysical properties of the food and the rubber cap are different. The same happens near the bottom of the food sample, due to the proximity with the steel.

The solutions of the one dimensional heat transfer models have been used to calculate the final enzymatic activity, also achieving very similar results to when the temperature of the two dimensional models are used. Therefore, as the one dimensional models are less complex and need less computational time to be solved, they can be suitable for optimization procedures.

The one dimensional models can be very useful to identify pressure and temperature dependent thermophysical parameters of these processes, by means of solving inverse problems related to the one dimensional model, which is once again simpler than considering the higher dimensional model.

Bibliography

[1] J. Aguilar Peris, *Curso de Termodinmica.* Alhambra Universal, 1986.

[2] Encyclopedia Britannica, 15^{th} Edition. 1989. Web: http://www.britannica.com/

[3] H. Bateman, A. Erdelyi, *Tables of Integral Transforms.* Vols. 1 and 2, McGrawHill Book Co., New York, 1954.

[4] J. C. Cheftel, *Review: high-pressure, microbial inactivation and food preservation.* Food Science Technology International 1 (1995) pp. 75–90.

[5] A. C. Cleland, R. L. Earle, *Assessment of freezing time prediction methods.* Journal of Food Science, 49. pp. 1034–1042.

[6] C. Dogan, O. Erkmen, *High pressure inactivation kinetics of Listeria monocytogenes inactivation in broth, milk, and peach and orange juices.* Journal of Food Engineerin 62 (2004) pp. 47-52.

[7] O. Erkmen, C. Dogan, *Kinetic analysis of Escherichia coli inactivation by high hydrostatic pressure in broth and foods.* Food Microbiology 21 (2004) pp. 181-185.

[8] A. Ibarz Ribas, G. V. Barbosa-Cánovas, *Operaciones unitarias en la ingenieria de alimentos.* Publicado por Mundi-Prensa Libros, 2005. ISBN 8484761630, 9788484761631. pp. 505-508.

[9] I. Indrawati, L. R. Ludikhuyze, A. M. van Loey and M. E. Hendrickx: *Lipoxygenase Inactivation in Green Beans (Phaseolus vulgaris L.) Due to High Pressure Treatment at Subzero and Elevated Temperatures.* J. Agric. Food Chem. 48 (2000) pp. 1850–1859.

[10] J. A. Infante: Anlisis numrico de modelos matemticos y problemas inversos en tecnologa de alimentos. Ph. D. Thesis, Universidad Complutense de Madrid, November 24, 2009.

[11] J. A. Infante, B. Ivorra, . M. Ramos and J. M. Rey, *On the Modelling and Simulation of High Pressure Processes and Inactivation of Enzymes in Food Engineering.* Mathematical Models and Methods in Applied Sciences (M3AS), Vol. 19, No. 12, (2009) pp. 2203–2229.

[12] L. R. Ludikhuyze, I. Van den Broeck, C. A. Weemaes and M. E. Hendrickx, *Kinetic parameters for pressure-temperature inactivation of bacillus subtilis α-Amylase under dynamic conditions.* Biotechnol. Prog. 13 (1997) pp. 617–623.

[13] L. Ludikhuyze, I. Van den Broeck, C. Weemaes, C. Herremans, J. F. Van Impe, M. E. Hendrickx, P. Tobback, *Kinetics for Isobaric-Isothermal Inactivation of Bacillus subtilis α-Amylase.* Biotechnol. Prog. 13 (1997) pp. 523–538.

[14] B. Ly-Nguyen, A. M. Loey, C. Smout, S. E. zcan, D. Fachin, I. Verlent, S. Vu Truong, T. Duvetter and M. E. Hendrickx, *Mild-heat and high-pressure inactivation of Carrot Pectin Methyl-esterase: A kinetic study*, J. Food Science 68 (2003), pp. 1377–1383.

[15] K. Miyagawa and K. Suzuki, *Studies on Taka-amylase A under high pressure: Some kinetic aspects of pressure inactivation of Taka-amylase A*, Arch. Biochem. Biophys. 105 (1964) pp. 297–302.

[16] M. Necati zisik, *Boundary Value Problems of Heat Conduction.* Dover Publications, Inc. New York, 1968.

[17] L. Otero, A. Ousegui, B. Guignon, A. Le Bail, P. D. Sanz, *Evaluation of the thermophysical properties of tylose gel under pressure in the phase change domain.* Food Hydrocolloids 20 (2006), pp. 449–460.

[18] L. Otero, P. D. Sanz, *High-Pressure Shift Freezing. Part 1. Amount of Ice Instantaneously Formed in the Process.* Biotechnol. Prog., 16 (2000), pp. 1030–1036.

[19] L. Otero, P. D. Sanz, *High-Pressure Shift Freezing. Part 2. Modeling of Freezing Times for a Finite Cylindrical Model.* Biotechnol. Prog., 16 (2000), pp. 1037–1043.

[20] L. Otero, P. D. Sanz, *Some Interrelated Thermophysical Properties of Liquid Water and Ice I. A user-friendly modeling review for food high-pressure processing.* Critical Reviews in Food Science and Nutrition, 42(4) (2002), pp. 339–352.

[21] L. Otero, P. D. Sanz, *Modelling heat transfer in high pressure food processing: a review.* Innovative Food Science and Emerging Technologies, 4 (2003), pp. 121–134.

[22] L. Otero, P. D. Sanz, *High-pressure-shift freezing: Main factors implied in the phase transition time.* Journal of Food Engineering, 72 (2006), pp.354–363.

[23] L. Otero, A. M. Ramos, C. de Elvira, P. D. Sanz, *A model to design high pressure processes towards a uniform temperature distribution.* J. Food Eng. Vol. 78 (2007) 1463–1470.

[24] J. P. P. M. Smelt, *Recent advances in the microbiology of high pressure processing.* Trends in Food Science and Technology **9** Elsevier (1998), 152–158.

[25] K. Suzuki and K. Kitamura, *Inactivation of enzyme under high pressure: Studies on the kinetics of inactivation of* α*–amylase of bacillus subtilis under high pressure*, J. Biochem. 54 (1963), pp. 214–219.

[26] Q. Tuan Pham, *Modelling heat and mass transfer in frozen foods: a review.* International Journal of Refrigeration, 29 (2006), pp. 876–888.

[27] U.S. Food and Drug Administration. Center for Food Safety and Apllied Nutrition, *Kinetics of Microbial Inactivation for Alternative Food Processing Technologies.* 2000. (Web: `http://www.cfsan.fda.gov/∼comm/ift-over-html`)

[28] H. F. Weinberger, *A first course in Partial Differential Equations* Dover, 1995.

[29] R. Xiong, G. Xie, A. E. Edmondson, M. A. Sheard, *A mathematical model for bacterial inactivation.* International Journal of Food Microbiology **46** Elsevier (1999), 45–55.